LASER INTERFEROMETER GRAVITATIONAL WAVE OBSERVATORY
-LIGO-
CALIFORNIA INSTITUTE OF TECHNOLOGY
MASSACHUSETTS INSTITUTE OF TECHNOLOGY

Technical Note	**LIGO-T0900128- v2**	4/28/09

Scattered Light Loss from LIGO Arm Cavity Mirrors

William P. Kells

This is an internal working note
of the LIGO Project.

California Institute of Technology
LIGO Project – MS 51-33
Pasadena CA 91125
Phone (626) 395-2129
Fax (626) 304-9834
E-mail: info@ligo.caltech.edu

Massachusetts Institute of Technology
LIGO Project – MS 20B-145
Cambridge, MA 01239
Phone (617) 253-4824
Fax (617) 253-7014
E-mail: info@ligo.mit.edu

WWW: http://www.ligo.caltech.edu

File /home/Kells/documents/T9000xx.ps – printed September 20, 2004

INTRODUCTION

For LIGO we are much interested in the fraction of incident [prescribed Gaussian mode beam] light lost ("scattered" out) from the mode when it is reflected from a mirror surface. Images of this light, from various non-specular view points, are by now familiar (figure 1). The apparent *statistical* homogeneity of the luminosity is striking which we adopt as a principle in our analysis. Guidance is given by the closely related theory of [statistically homogeneous] "laser speckle" scatter[1]. However nominally that theory applies to *rough* surfaces (surface point-point height variations $>\lambda_0$), in which case all incident light is scattered (no specular beam). For LIGO surfaces, residual surface "micro"-roughness is anticipated (via fabrication epoch metrology) to be shallow ($\ll\lambda_0$)[2]. In addition we know operationally that the loss fraction is $\ll 1$ and the specular mode is essentially the incident. This suggests a perturbative analysis where the mean scatter field is on order the first [scaled dimensionless] moment of the inhomogeneity, that is σ/λ_0.

Of course only surface *inhomogeneities* scatter (we *define* thus). Therefore loss cannot be uniformly distributed and a local "speckle" character (Fig. 1) is to be expected. Such generic character cannot inform whether the inhomogeneities are non-perturbative point-like (size <imaging resolution) or true locally random micro-roughness. Distinguishing these categories is vital for LIGO since they likely arise from different phases of mirror fabrication. The former may be regarded as [potentially curable] point *defects* since they are known to be sporadic on sufficiently high quality mirrors. Here we derive signatures of perturbative of homogeneous micro-roughness scatter in order to distinguish (and quantify) any point defect component. Accumulated evidence (in situ scatter measurements as presented here; higher than anticipated total LIGO arm cavity losses; and laboratory surface scatter loss scans)[7] indicates that point defects (including surface contamination) strongly contribute to net mirror loss.

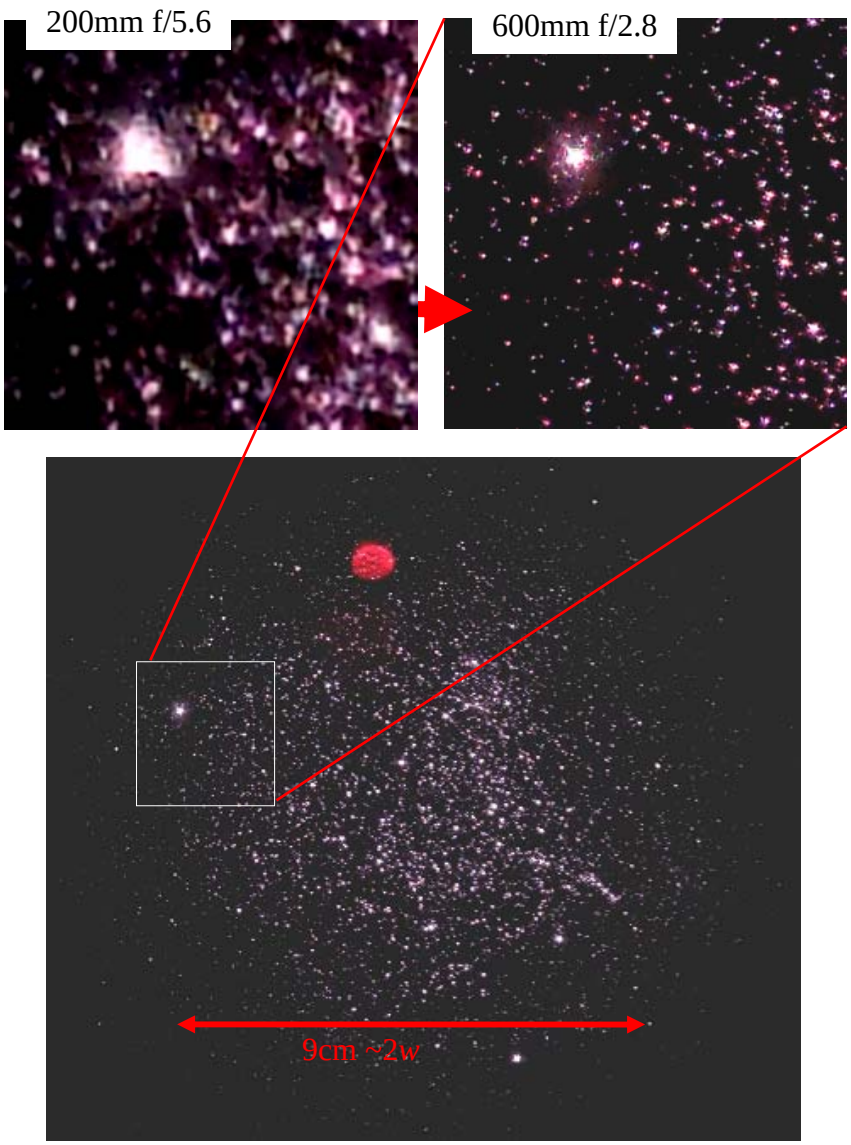

Figure 1. High resolution images of the beam spot on LIGO ETM mirror. The apparent "globular cluster" shape is due to the Gaussian surface illumination. It is clear that certain extreme bright points are flaws. Otherwise the "star" sizes are consistent with diffraction limited imaging optics. The view point used for this imaging is the highlighted in Fig. 3

Connection to "laser speckle" scatter.

Under the assumption that the extremely regular surface (polish+coating) quality of interest (~ LIGO mirrors) is homogeneous in an ensemble mean sense we can analyze the statistical properties of coherent light scattered from specimens of the ensemble. The field of a finite (*w* Gaussian width) beam scattering from such specimens was developed[2], which we use as our starting point. Since the relevant surface area is finite (LxL~$4w^2$), it is convenient to approximate it as a matrix of NxN coherently scattering pixels (N sufficiently large that $L/N \rightarrow < \lambda_0$). Already in that primary analysis the "golden rule" net loss formula was re-derived (conditions of validity discussed):

$$P_{scatter} \approx P_0 \,|\, 4\pi\sigma_{eff} / \lambda_0 \,|^2 \qquad (1)$$

Features of this lumped loss will only be referred to. Instead here the main goal is to elucidate the intensity distribution, as illustrated in figure 1, using the same DFC beamlet, representation of the scatter field. The essential feature of describing the diffraction scatter in this way is that then it appears analogous to the established statistical description of "laser speckle" scatter[1]. Many characteristic "speckle" results analogously emerge. These give clean predictions for properties of images (e.g. figure 1) whose comparison to observations indicates the character of surface distortion.

We summarize the essentials of speckle scatter theory[1]. The pixels which the scattering surface is divided into are considered be of individually random height $h_{\mu,\nu}$ (over interval $\geq \pm\lambda_0$, hence *rough*) from a specular reference surface. Statistically it is vanishingly unlikely that any such specimen surface distortion would be isotropic. However *ensembles* of them are both isotropic and homogeneous. In this special, *completely* random case the specular reference surface shape (spherical, flat, etc) as well as the extent (L) of this rough distortion (as long as L> incident beam size) are irrelevant. Even the pixel size (L/N) is not crucial (needs not $\rightarrow < \lambda_0$) as long as a statistically sufficient number fill the illuminated area (or object Airy patch for imaging analysis, see below). The field reflected from such specimens is evaluated at any distant observation point ***r*** as the sum over [~equal magnitude] random phasors representing each pixel[2]. The ensemble mean square of these sums (intensity when obliquity is separately factored in) is the same for any ***r***. Therefore there is no distinguishable *specular* reflection, and the incident power, $\mathbf{P}_0$, is all scattered with mean intensity $\mathbf{P}_0\cos\theta/\pi r^2$ (polar θ from incident, there being no azimuthal dependence in this *scalar* treatment). Of course, for any one specimen the intensity is distributed as randomly as the specimen pixels are.

The value of analyzing in terms of a large number of randomly independent pixel/phasors is that the central limit theorem (CLT) may be invoked to predict likelihood distributions for physical quantities of interest for *likely* specimens (examples of which it is assumed we are always dealing with). For example the field amplitude distribution [over the ensemble] is Gaussian via the CLT. This implies that the intensity distribution is $\propto e^{-I/I_0} dI$ (I_0 being the mean given above), so that the most likely intensity at any point is zero. This describes the characteristic spatial intensity fluctuation of speckle (quantitatively confirmed experimentally).

The speckle "size" (2 point correlation width) is also predicted. The correlation angle δθ between two far field points (**P-P′,** figure 2) is $\lambda_0 / 4w$ so that the speckle "size" is~ $r\lambda_0 / 4w$. Note that this is the same as the Airy disc width of a constant amplitude illuminated aperture radius ~w (a first Fresnel zone*)*. The form of the speckle field may be thought of as a superposition of isotropically distributed such Airy disc amplitudes each of random phase. Also, speckle may be observed in telescopic (field lens, D and fl, normal to ***r*** at any **P**/**P′**) images of the illuminated scattering surface.

Such images must consist of intensity features no smaller than the Airy radius $\rho_A \sim f l\lambda_0 / D$, resolving only "object" (scattering surface) patches of radius $d_A/2 \sim r\lambda_0 / D >> L/N \sim \lambda_0$. Therefore adjacent patches are randomly different, and their adjacent image spots of randomly different intensity. Thus the image speckles are of mean size ρ_A(evidently the "stars" of Fig 1).

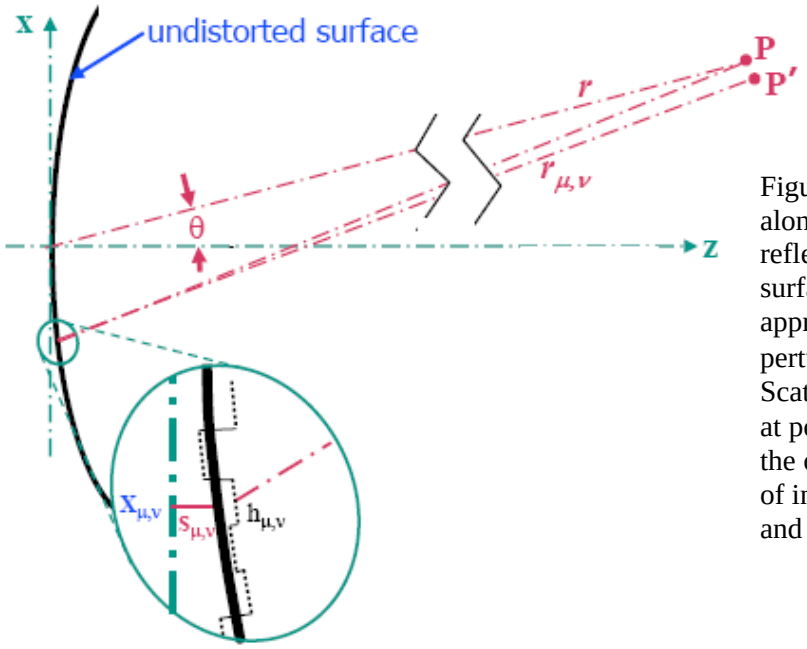

Figure 2. Beam incident along z axis) perfectly reflects from specular surface by distortion approximated by pixel perturbations $h_{\mu,\nu} << \lambda_0$. Scatter field is observed at points $\mathbf{P}(r)$, $\mathbf{P}'(r)$ w.r.t the origin (intersection of incident beam axis and undistorted surface).

Differences with "laser speckle" scatter.

Although actual images (Fig. 1) and the plausibly random residual surface roughness of LIGO-like mirrors suggest a speckle analogy, three major differences make any direct application of the above results unclear. First, the distortion (pixel) height scale is far ($\ll \lambda_0$) from being rough[2], with, e.g. the conspicuous qualitative consequence that there is a dominant specular reflection. Second, although at least qusi-homogeneous, it is known that otherwise flawless precision polishing results in a fractal power spectrum of residual distortions[3,4]. This means that the scatter (even in the ensemble average) can only be *azimuthally* isotropic, whereas completely random pixels would scatter (in the mean) uniformly in all directions. That is, there are strong long range correlations amongst the $h_{\mu,\nu}$ of any realistic polished surface even if regarded as being homogeneous. Third, closely related to this, is the fact that a true fractal homogeneous distortion ensemble is not possible for the finite specimen mirrors actually fabricated. There is always some surface scale at which the homogeneity and isotropy break down[3]. Some results (e.g. total loss, Eqn. 1) which include scattering from all scales will remain intrinsically uncertain in any statistical analysis[5].

Perturbative beamlet speckle scatter.

A perturbative random ensemble description of micro-roughness (e.g. LIGO-like) scattering is developed in analogy to the canonical speckle theory, naturally incorporating these differences. Fresnel-Kirchhoff diffraction, expressed to $\mathcal{O}(\mathrm{h}_{\mu,\nu}/\lambda_0)$ as discreet sums over radiation from the surface pixels, gives the [far] **P**(*r*) field. For LIGO-like parameters (*w*/ROC<<1, $|\mathrm{h}_{\mu,\nu}|/\lambda_0 \ll 1$), each DFC of the pixel array (N^2 over L^2) distortion becomes the coefficient $\tilde{\mathrm{h}}_{\mathrm{m,n}}$ of a diffracted Gaussian *beamlet* propagating in the grating direction $\hat{\mathbf{k}}_{m,n}$ corresponding to that DFC. This is an accurate representation assuming 1. neglect of aberration terms $\mathcal{O}(w/ROC)^2$ 2. first order in the perturbation $\mathcal{O}(\mathrm{h}/\lambda_0)$; 3. scalar wave approximation; and 4. paraxial description of the beamlets[3]. This decomposition allows for arbitrary beamlet [magnitude] spectrum (within the constraint of assumption 2. and Parseval's condition), accommodating any presumed (e.g. fractal) distortion and anisotropic scatter intensities. Restriction to *homogeneous* distortion ensembles requires these coefficients be of mutual random *phase*. This *phase* randomness provides the direct analogy to pixel *height* randomness in canonical speckle theory.

The coefficient $\tilde{\mathrm{h}}_{0,0}$ DFC is the specular diffraction at θ=0 which we avoid by observing only at large angles (θ >.017 Rad, or $\tilde{\mathrm{h}}_{\mathrm{m,n}}$ where n,m > 1800). This practically avoids ambiguous treatment of small angle (large surface scale: 3^{d} caveat above) region. Figure 1 is at a typical accessible observation point, with θ =0.16 and *w*<<*r*~5m<<r_{Ray}. Thus any beamlet subtends dθ<*w*/r<<θ so that only a small fraction dk/k of the DFC spectrum contributes at this point. For reasonable ensemble spectra we can then approximate contributing $|\tilde{\mathrm{h}}_{\mathrm{m,n}}|$ to be constant. On the other hand this contributing band of DFCs all interfere with random phases and are sufficiently numerous (~$(4w^2/\lambda r)^2$~ 10^6) to invoke the same statistical argument used for canonical speckle. The *mean* intensity in this direction is just its central beamlet power divided by its [Gaussian *w*] area at **P**, and distributed with exponential probability (same as for speckle). Similarly the *mean* size of the speckle is given by the angle (**P-P′**) over which the particular interference coheres ~$\lambda_0/4w$[6]. In this discussion the "*w*" used is strictly the beamlet Gaussian width at *r*. However for Fig.1 (and all directly accessible observation points) r <<r_{Ray} so that there is negligible **O-P** variation in *w*.

This result may be used to resolve a crucial experimental question. The original (and by now considerable) data measuring the LIGO arm cavity mirror scatter consisted of monitoring the net power impinging on a PD (area or collecting lens a^2) placed at **P** (Fig. 3,normal to ***r***)[7]. Practical constraints require this PD **P** to remain fixed, so there has been no attempt to point sample the field to establish [local] mean I_0. However it

has been presumed that these PD measurements are accurately proportional to this *mean* scatter field intensity for their θ location. Since we observe only a specimen, this can only be valid if a is sufficiently large. Now we understand the criteria for accurate mean PD samping to be that "statistically many speckles fall within PD collection area" or > $(2aw/\lambda r)^2 \sim 4x10^3$ for the above case[8]. This criterion for uniform PD response is essentially the same as described above for [rough surface] speckle, the only difference being in the definition of "*w*". Therefore any [additional] scatter contribution from rough "point" defects would be also be uniformly sampled as long as there are statistically many of them within the mirror beam spot.

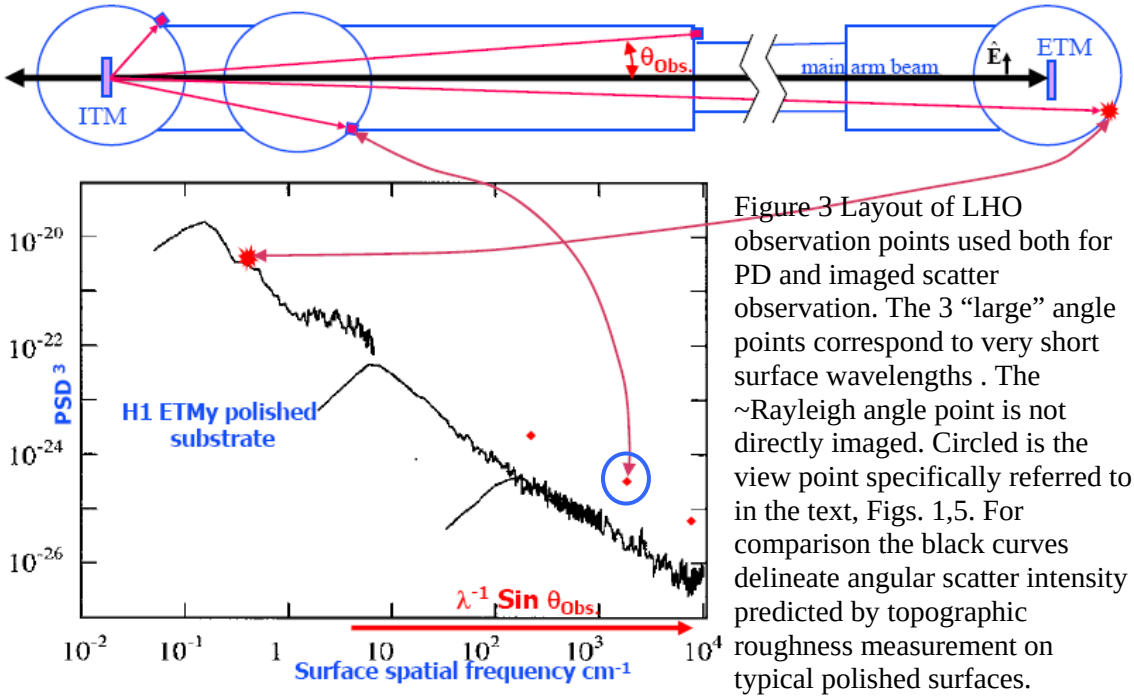

Figure 3 Layout of LHO observation points used both for PD and imaged scatter observation. The 3 "large" angle points correspond to very short surface wavelengths . The ~Rayleigh angle point is not directly imaged. Circled is the view point specifically referred to in the text, Figs. 1,5. For comparison the black curves delineate angular scatter intensity predicted by topographic roughness measurement on typical polished surfaces.

Imaged micro-roughness scatter.

Qualitatively, the circumstances and appearance of images (Fig. 1) of optic surfaces at non-specular θ_{Obs} have striking "laser speckle"resemblence. To quantify this, first recall that any imaging system cannot display features finer than the Airy disc ($2\rho_A = 1.2\lambda_0$[fl/D], "diffraction limited" for telescope aperture D, f# =[fl/D]). This corresponds to an Airy "patch" (diameter $d_A = 1.2r\lambda_0/D$) on the object whose pixels contribute entirely unresolved to an image Airy disc amplitude. For all imaging configurations investigated in LIGO, $d_A > 0.1$mm so that isolated "point" defects are highly unresolved, appearing as Airy "stars" of Fig.1. The field of any particular "$\mathbf{d_A^2}$" patch may expressed as a sum of the radiation from each of the surface pixels **(μ,ν)** it contains:

$$\propto \frac{qE_o(\mathbf{x}_{\mu,\nu})e^{i2\pi \mathrm{h}_{\mu,\nu}}}{r_{\mu,\nu}} e^{i2\pi|\mathbf{x}_{\mu,\nu}+(\mathbf{s}_{\mu,\nu}+\mathrm{h}_{\mu,\nu})\hat{\mathbf{e}}_z+\mathbf{r}|/\lambda_0} \qquad (\boldsymbol{\mu}, \boldsymbol{\nu}) \in \mathbf{d}_{\mathrm{A}}^2 \tag{2}$$

where we follow closely the derivation of [3] (Eqns.12-16). Since PD detection (last section) sees *all* surface pixels it was necessary to represent the sum over (2) as beamlet contribution from all pixels. Here the restriction to pixels only *within* $\mathbf{d}_{\mathrm{A}}^2$ allows simplification of the form of (2) over contributing pixels. For imaging to be quantitatively interesting we want to resolve surface features $d_A << w$. The Gaussian optics of the undistorted cavity surfaces is such that $w \geq \sqrt{\lambda_0 ROC}$. Therefore the local undistorted surface sag across d_A is $<<\lambda_0$, itself perturbative. Further, the condition $d_A << w$ allows $E_0(\mathbf{x}_{\mu,\nu})$ of (2) to be approximated as constant across $\mathbf{d}_{\mathrm{A}}^2$. Considering now only micro-roughness, the patch contains no rough ($h_{\mu,\nu} \sim \lambda_0$) defects, allowing the sum of these pixel contributions to the field of $\boldsymbol{\rho}_{\mathrm{A}}^2$ to be written as:

$$\mathrm{C}_\theta \frac{E_o(\mathbf{d}_{\mathrm{A}}^2)}{|\mathbf{x}_{\mathbf{d}_{\mathrm{A}}^2}+\mathbf{r}|} \sum_{\mu,\nu \in \mathbf{d}_{\mathrm{A}}^2} (\lambda_0 + \mathrm{h}_{\mu,\nu} + \delta \mathrm{s}_{\mu,\nu}) e^{i2\pi|\mathbf{x}_{\mu,\nu}+\mathbf{s}_{\mu,\nu}+\mathbf{r}|/\lambda_0}$$

$$\mathrm{C}_\theta \equiv \frac{i2\pi(1+\cos\theta)\mathrm{L}^2}{\lambda_0 \cos\theta N^2} \tag{3}$$

Where $\delta s_{\mu,\nu}$ is the local sag w.r.t. a mean tangent plane in $\mathbf{d}_{\mathrm{A}}^2$. Proceeding as in Ref. 3, the specular ($\sim\lambda_0$) term is ignored and perturbative terms (h and δs) are represented by DFCs:

$$\mathrm{C}_\theta \frac{E_o(\mathbf{d}_{\mathrm{A}}^2)}{|\mathbf{x}_{\mathbf{d}_{\mathrm{A}}^2}+\mathbf{r}|} (\tilde{\mathrm{h}}_{m,n} + \widetilde{\delta \mathrm{s}}_{m,n}) e^{i2\pi|\mathbf{r}_{\mathbf{d}_{\mathrm{A}}^2}|/\lambda_0} \sum_{\mu,\nu \in \mathbf{d}_{\mathrm{A}}^2} e^{i(\hat{\mathbf{k}}_{\mathrm{m,n}} - \hat{\mathbf{k}}_\theta)(\boldsymbol{\mu},\boldsymbol{\nu})} \tag{4}$$

where $|\mathbf{r}_{\mathbf{d}_{\mathrm{A}}^2}|$ is the local distance to the observation point and $\hat{\mathbf{k}}_\theta \approx 2\pi \hat{\mathbf{r}} \mathbf{x}_{\mu,\nu}/\lambda_0 \equiv 2\pi \sin\theta(\boldsymbol{\mu},\mathbf{0})\mathrm{L}/\mathrm{N}\lambda_0$ is the "grating" directional vector at the [polar] observation point angle θ_{Obs}. Since $\delta s_{m,n}$ represents the undistorted locally nearly flat surface shape, all its DFCs are negligible at θ_{Obs} of interest ($>>\lambda/2w$). The sum in (4) is ~zero unless $|\hat{\mathbf{k}}_\theta - \hat{\mathbf{k}}_{m,n}| < \lambda_0/d_A$, so that only a narrow band, $\boldsymbol{\Delta}(\mathbf{n},\mathbf{m})$, where $|\tilde{\mathrm{h}}_{\mathrm{m,n}}| \approx \mathrm{Const}$, contributes to $\boldsymbol{\rho}_{\mathrm{A}}^2$: Summing over all such non-negligible components gives the net amplitude of $\boldsymbol{\rho}_{\mathrm{A}}^2$:

$$\approx \mathrm{C}_{\theta}\frac{E_o(\mathbf{d}_{\mathrm{A}}^2)}{|\,\mathbf{x}_{\mathbf{d}_{\mathrm{A}}^2}+\mathbf{r}\,|}|\tilde{\mathrm{h}}_{m,n}|\,e^{i2\pi|\mathbf{r}_{\mathbf{d}_{\mathrm{A}}^2}|/\lambda_0}N_{\mathbf{d}_{\mathrm{A}}^2}\sum_{\Delta(\mathbf{m},\mathbf{n})}e^{i\varphi_{m,n}} \qquad (5)$$

where the [ensemble] random phases, necessary for homogeneity, of each DFC are displayed and $N_{\mathbf{d}_{\mathrm{A}}^2}$ are the number of pixels within $\mathbf{d}_{\mathrm{A}}^2$. For given camera vantage and settings all factors in (5) except the sum are practically constant or vary smoothly (E_0 and $\mathbf{r}_{\mathbf{d}_{\mathrm{A}}^2}$ phase) across the beam image. These determine systematic position *mean* brightness within the image. Locally however, at each $\boldsymbol{\rho}_{\mathrm{A}}^2$ the sum is Gaussian random since a large number, $\mathcal{O}(\mathrm{L}/\mathrm{d}_{\mathrm{A}})^2 \geq 10^4$ (analyzed images, e.g. Fig. 1,5) **(m,n),** contribute[10,11]. These conditions imply locally the same (exponential) image intensity statistics as held for canonical rough speckle. We conclude that small neighborhoods in micro-roughness scatter images appear the same as equivalently imaged rough speckle fields.

We note that such imaged speckle (rough or micro) does not appear as an invariant pattern, except for geometrical distortions, from any perspective. Follow the image of the same patch $\mathbf{d}_{\mathrm{A}}^2$ as the camera observation point rotates to $\theta \pm \delta\theta$. According to the criteria leading to (5) only **(m,n)** such that $|\hat{\mathbf{k}}_{\theta\pm\delta\theta} - \hat{\mathbf{k}}_{m,n}| < \lambda_0/\mathrm{d}_{\mathrm{A}}$ will contribute, and these bands will contain all different components (of randomly different phase) if $\delta\theta > \lambda_0/\mathrm{d}_{\mathrm{A}}$. Thus there is a $\delta\theta$ correlation angle outside of which images of the beam spot will appear statistically similar but have zero same surface point cross-correlation. Isolated "point" defects will have invariant image Airy discs since their DFC phases are completely correlated (prescribing their position).

Predictions for and analysis of images.

During the course of LIGO(Hanford) commissioning sporadic images[7,9] were taken under sufficiently controlled circumstances to apply simple quantitative processing techniques. For these the perturbative speckle interpretation (last section) should well apply, implying several predictions for images as a function of camera prameters (θ_{Obs}, *r*, camera f# and fl). Reliable data was limited to observations at a single *r* (~5-6m), however there was some flexibility on θ_{Obs} (within view port aperture; opposite beam tube sides). The goal of this quantitative image analysis is to distinguish any violation of these micro-roughness regime predictions indicating significant (w.r.t. loss) point defect scattering. Indications of excess cavity loss (operational and corroborated by TIS mirror surface scans) plus the large angle point-like PD data excess in Fig. 3 motivates this pursuit[12].

First we consider fixed θ_{obs} images (leaving only camera f#, fl variable). The quantitative technique is to histogram the CCD pixel values ("intensities") as in figure

5. In all cases the CCD "pixel scale" is $<<\rho_A$. Data fields are cropped from full images corresponding to ~uniform beam illumination ($|E_o(\mathbf{d}_A^2)| \approx Const.$), yet still contain a large statistical sample of speckle (*crop*$>>\rho_A$). Under these circumstances, CCD pixel intensity values imaging homogeneous micro-roughness will mimic the probability distribution for $\boldsymbol{\rho}_A^2$ derived above: $dn(I) \propto N_{Tot} e^{-I/\langle I \rangle} dI$, with mean image intensity:

$$\langle I \rangle_{\text{camera Obs. } \theta} \propto P_0 \left\langle |\tilde{h}_{m,n}|^2 \right\rangle_{(\mathbf{m},\mathbf{n}) \in \mathbf{k}_{Obs}} (f_\#)^{-2} \tag{6}$$

Therefore, as long as a significant sample of speckle are resolved in the cropped image, the distribution of intensity depends *only* on f#. This allows close comparison of images where f# is varied via lens aperture setting (same fl lens). In comparison, "point" defects are not resolved so that their apparent ($\boldsymbol{\rho}_A^2$ peak) intensity is:

$$I_{\text{Peak}} \propto P_0 \left(\frac{\text{fl}}{r} \right)^2 (f_\#)^{-4} \tag{7}$$

According to (6-7) any point component may be discriminated by comparing image pixel histograms at various f#. This is schematized in figure 4, making clear that any intense image points eventually loose contrast against a "sea" of background speckle as $f\# \to \infty$ [10]. Sufficiently low resolution (high f#) images were found to follow the exponential distribution within statistical resolution[7]. Figure 5 analyzes a central crop of the same image shown in Fig 1, representing our highest resolution data. A

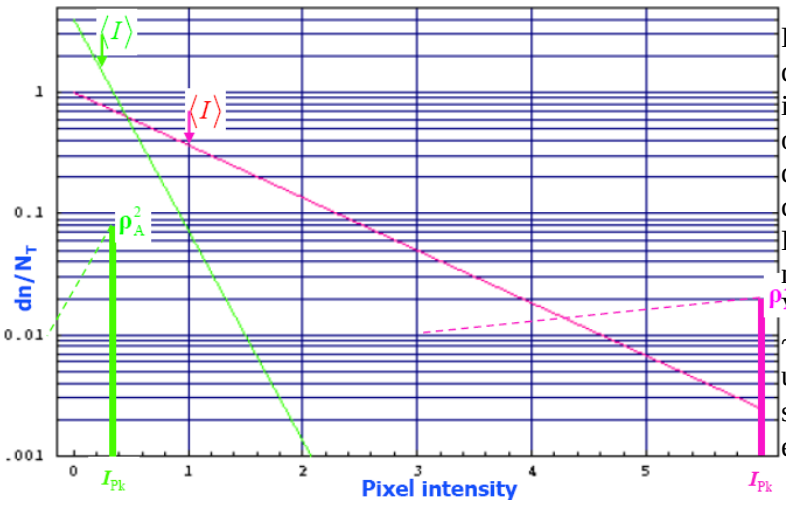

Figure 4. Comparison of distributions of CCD pixel intensities for same imaged object area. Pink and green distributions differ only in camera f# value (f# =2f#). Exp[-*I*/<*I*>] lines represent micro-roughness speckle. Vertical bars represent ~peak bins from isolated unresolved point defect scatter. $f\# \to 0$ greatly enhances the point contrast

dominant point component is indeed resolved. However since this image is taken at a large $|\hat{\mathbf{k}}_{m,n}|$ numerical "angle", micro-roughness contributes with weight $\propto |\tilde{h}_{n,m}|^2 / |\mathbf{k}|$ (<<1 at large angle points in Fig. 3) relative to ~isotropic point

scatter. Much of the spectrum (e.g. small $|\hat{\mathbf{k}}_{m,n}|$,* point in Fig.3), unfortunately not accessible to imaging, is evidently dominated by micro-roughness. Thus this current level of image analysis does not have sufficient angular (spectral) coverage to determine the point defect *loss* fraction. However, these large angle observations are ideal diagnostics of point defects yielding high contrast images of their density and distribution.

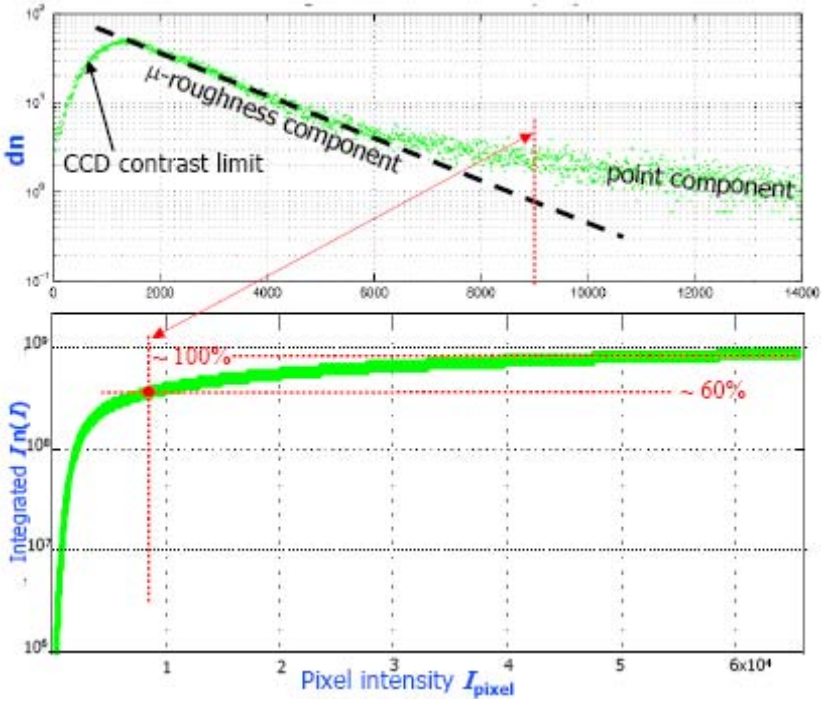

Figure 5 High resolution histogram (top) of central crop of Fig. 1 image (f#2.8). CCD/readout limitations roll u-rough exponential off at low intensity. Intensity weighted integrated (bottom) histogram used to evaluate point component as ~90% of total scattered light at this θ_{Obs}.

Second, we investigate how images at different observation points (angle only, so that image resolution is invariant) are correlated. Here we ignore beamlet aberration affects (predictably removable from correlations), and assume the incident beam position and intensity is constant (scattering source invariant). It was pointed out that (5) implies a correlation angle $\delta\theta < \lambda_0 / d_A$ for pure (homogeneous) micro-roughness images scatter. But this corresponds to a lateral shift in camera position, $r\delta\theta < D_{lens}$. That is, shifting the camera laterally by greater than one aperture diameter should yield locally randomly different image speckle patterns[11]. LIGO observation ports accommodate checking this since their aperture is several times that of typical lenses. For θ_{Obs} corresponding to Fig1,3,5 strong image correlation was found beyond this limit. This is consistent with the dominance of the point component found in Fig. 5 (and corresponding points in Fig. 3). Given the anticipated steep spectrum for $|\tilde{h}_{m,n}|$ (Fig.3) substantial de-correlation would be expected over images at very small θ_{Obs}. However this regime is practically inaccessible to the LIGO configuration (Fig.

3). Since the images are in stable digital format it would be straightforward to systematically (say as a function of $\delta\theta$) calculate intrinsic (local) cross correlations, normalizing out extraneous DOFs (exposure/illumination changes; view point aberrations, registration, etc.).

REFERENCES:

1. J. Goodman, in Laser Speckle and Related Phenomena, Topics in Applied Physics Vol. 9, 2nd Ed. Springer, 1984.

2. On small scales $\leq$ mm polished surfaces with random rms roughness $\leq$ nm can be achieved. Then on long scales (up to the substrate diameter) systematic distortions ("aberrations") can also be held to $\leq$ nm amplitudes. On the other hand any process will have some [random] frequency of flaws, typically "point" (in experience $\approx \mathcal{O}$(pixel) width) defects. These cannot be assigned a perturbative ($|h_{\mu,\nu}| / \lambda_0 \ll 1$) pixel height $h_{\mu,\nu}$, and therefore are not considered here in the micro-roughness analysis. It is a hypothesis that the ensemble of such defects contributes insignificantly to loss. This is to be tested against the statistical predictions from random micro-roughness alone.

3. W. Kells, LIGO-T070310-v1.

4. E. Church, P. Takacs, (and Leonard, SPIE Vol 1165); Handbook of Optics, Vol I; and SPIE Vol 645.

5. Equation (1) is a clear example, attempting to express loss as a function of any σ^2, a *statistical* measure of the surface roughness. The general problem with exactly doing so was emphasized in reference 3. For fractal like surface structure (even if random and homogeneous) σ^2 has no fixed value but varies with L, typically diverging as $L \to \infty$. The natural L~(incident beam width) can be approximately adopted to define a σ^2_{Leff} however this is still ambiguous since diffraction (scatter field amplitude) is over [weighted] Fourier components of the roughness. No abrupt truncation of components (L^{-1}_{eff}) is equivalent. It is sometimes proposed that an "incident beam intensity (e.g. Gaussian) weighted σ^2_h" is the correct quantity to use in (1). This leaves just as ill-defined the sampling prescription for local measure of σ^2_h. Practically the concept is useful only for better predicting loss for characteristically *inhomogeneous* surfaces.

6. Here we use the identity that, as $N \to \infty$, $\sum_{n=0}^{N} e^{i\varphi_n}$ and $\sum_{n=0}^{N} e^{i\varphi_n} e^{i2\pi n/N}$ are completely uncorrelated for random φ_n.

7. W. Kells LIGO-G080078,….. Note that *indirect* measurement of scatter intensity was also inferred at one extremely small $\theta \sim \theta_{Ray}$ (V. Frolov,et al, LLO i-log, 2006) Indeed this was observed to be in a regime where the intensity was spatially irregular, making an interpretation of mean I_0 highly uncertain.

8. The PDs (or their collection lens) were selected before this criteria was appreciated. It is fortuitous that the combination of PDs and observation points has been consistent with uniform scatter loss sampling. However the worst case sampling has been $n_{speckle} \leq 100$, and this only because relatively large area PDs (> mm^2) have been used.

9. Practically all quantitative imaging involved view ports such that θ_{Obs} =8-9^o(e.g. Fig 1). This allowed for high resolution with reasonable f# lenses, yet angles small with respect to aberrations (Cosθ=1) and large with respect to Rayleigh. Available view port geometry accessed only "P" polarization scatter (the LIGO beams are horizontally polarized). A full vector description of scatter (from even statistically azimuthally isotropic surfaces) then predicts azimuthal dependence (but only in brightness, not speckle character, and no more than a 1% correction from scalar for θ_{Obs} discussed here).

10. Eventually, as f# increases the entire image becomes one, unresolved, Airy disc and (6) breaks down (as it must eventually go as ~r^{-2}). This indicates that any distinction between micro-roughness and point scattering perturbations ceases to have meaning. Distinguishing point defects depends on their scattering amplitude dominating the net contribution to some $\boldsymbol{\rho_A^2}$. This contrast diminishes as the relative contribution of micro-roughness increases in proportion to $\mathbf{d_A^2}$. Even with no such competing micro-roughness any statistically significant N_{point} distributed on the surface will appear indistinguishable from speckle as $f\# \to \infty$ since the "isolated" points will begin interfering.

11. Given a fixed LxL discreet grid it would seem that $\mathcal{O}(L/d_A) \gg 1$ would break down. However, physically, over a realistic ensemble the field must retain the same random features as $r, d_A \to \infty$. Although fixed $L \geq 2w$ are sufficient to describe the net scatter (loss), the fixed grid pattern leaves non-random artifacts in the DFC description of the field. This can always be removed (to any far field angular scale) by formally employing a statistically equivalent surface with $L \to \infty$. This ensures $\mathcal{O}(L/d_A) \gg 1$ at any *r*, with Gaussian random field distribution. Similarly the de-correlation of image speckle upon lateral camera position shift $r\delta\theta$ >D cannot remain valid as D is reduced to a "pinhole" (<< far field un-imaged speckle width ~$r\lambda_0 / 4w$). The break down

in this “pinhole” limit entails the entire beam image coalescing into a single Airy disc with no correlatable structure.

12. H. Yamamoto, LIGO-T070082-03-E; W. Kells, LIGO-T080010, LIGO-T070051;

13. *Optics*, M. Klein, T. Furtak, 2nd Ed., pp. 468-476. See also the discussion in *Lasers*, A.Siegman, pp. 637-652. Note that the Fresnel propagation of Gaussian beam wave fronts described in these texts are approximate at the same (paraxial) level as made in the reduction of (14) to (16). The astigmatic aberrations due to beamlet inclination (θ) from normal are essentially the same as encountered in describing the non-normal incidence ($\theta/2$) reflection of a Gaussian beam as $\hat{\mathbf{k}}_{\theta/2}$[specular] diffraction, where we know that the diffracted is just an astigmatic Gaussian beamlet.